Influence of Arctic Microlayers and Algal Cultures on Sea Spray Hygroscopicity and the Possible Implications for Mixed-Phase Clouds

JGR Atmospheres

RESEARCH ARTICLE
10.1029/2020JD032808

Influence of Arctic Microlayers and Algal Cultures on Sea Spray Hygroscopicity and the Possible Implications for Mixed-Phase Clouds

Sigurd Christiansen[1], Luisa Ickes[2,3], Ines Bulatovic[2], Caroline Leck[2], Benjamin J. Murray[4], Allan K. Bertram[5], Robert Wagner[6], Elena Gorokhova[7], Matthew E. Salter[7], Annica M. L. Ekman[2], and Merete Bilde[1]

[1]Department of Chemistry, Aarhus University, Aarhus, Denmark, [2]Department of Meteorology and Bolin Centre for Climate Research, Stockholm University, Stockholm, Sweden, [3]Department of Space, Earth and Environment, Chalmers University of Technology, Gothenburg, Sweden, [4]Institute for Climate and Atmospheric Science, School of Earth and Environment, University of Leeds, Leeds, UK, [5]Department of Chemistry, University of British Columbia, Vancouver, British Columbia, Canada, [6]Institute of Meteorology and Climate Research, Karlsruhe Institute of Technology, Karlsruhe, Germany, [7]Department of Environmental Science, Stockholm University, Stockholm, Sweden

Abstract As Arctic sea ice cover diminishes, sea spray aerosols (SSA) have a larger potential to be emitted into the Arctic atmosphere. Emitted SSA can contain organic material, but how it affects the ability of particles to act as cloud condensation nuclei (CCN) is still not well understood. Here we measure the CCN-derived hygroscopicity of three different types of aerosol particles: (1) Sea salt aerosols made from artificial seawater, (2) aerosol generated from artificial seawater spiked with diatom species cultured in the laboratory, and (3) aerosols made from samples of sea surface microlayer (SML) collected during field campaigns in the North Atlantic and Arctic Ocean. Samples are aerosolized using a sea spray simulation tank (plunging jet) or an atomizer. We show that SSA containing diatom and microlayer exhibit similar CCN activity to inorganic sea salt with a κ value of ~1.0. Large-eddy simulation (LES) is then used to evaluate the general role of aerosol hygroscopicity in governing mixed-phase low-level cloud properties in the high Arctic. For accumulation mode aerosol, the simulated mixed-phase cloud properties do not depend strongly on κ, unless the values are lower than 0.4. For Aitken mode aerosol, the hygroscopicity is more important; the particles can sustain the cloud if the hygroscopicity is equal to or higher than 0.4, but not otherwise. The experimental and model results combined suggest that the internal mixing of biogenic organic components in SSA does not have a substantial impact on the cloud droplet activation process and the cloud lifetime in Arctic mixed-phase clouds.

Key Points:
- CCN activity of aerosolized Arctic sea surface microlayer and diatom cultures is similar to sea salt
- For accumulation mode aerosols, the simulated cloud properties do not depend strongly on κ unless κ is <0.4
- Aitken mode aerosols can sustain the simulated Arctic cloud, but only if κ is high, in this specific case ≥0.4

Supporting Information:
- Supporting Information S1

Correspondence to:
M. Bilde and A. M. L. Ekman,
bilde@chem.au.dk;
annica@misu.su.se

Citation:
Christiansen, S., Ickes, L., Bulatovic, I., Leck, C., Murray, B. J., Bertram, A. K., et al. (2020). Influence of Arctic microlayers and algal cultures on sea spray hygroscopicity and the possible implications for mixed-phase clouds. *Journal of Geophysical Research: Atmospheres*, *125*, e2020JD032808. https://doi.org/10.1029/2020JD032808

Received 23 MAR 2020
Accepted 27 JUL 2020
Accepted article online 26 AUG 2020

Author Contributions
Conceptualization:
Sigurd Christiansen, Luisa Ickes, Ines Bulatovic, Elena Gorokhova, Matthew E. Salter, Annica M. L. Ekman, Merete Bilde

1. Introduction

The Arctic region is currently warming faster than the rest of the globe (Blunden & Arndt, 2019), and as sea ice cover is diminishing (Blunden & Arndt, 2019), the effect of a potential increase in sea spray aerosol (SSA) emissions on clouds and climate calls for attention. Low-level mixed-phase clouds may play an important role in this enhanced warming due to their strong influence on the surface energy budget and their frequent occurrence throughout the year (e.g., Shupe & Intrieri, 2004). In contrast to many other regions, low-level clouds generally warm the surface of the Arctic, as the overall level of solar radiation is low and the surface is often covered by snow or ice. It is well known that aerosols affect clouds by acting as cloud condensation nuclei (CCN) or ice nucleating particles (INPs) (Boucher et al., 2013; Lohmann & Feichter, 2005), but CCN and INP properties of Arctic marine aerosols are currently not well characterized (Abbatt et al., 2019; Martin et al., 2011).

Due to the inaccessibility of the high Arctic (north of 80°) data from this region remain particularly sparse. Measurements of CCN were carried out throughout an icebreaker research expedition to the high Arctic during the biologically most active period in the summer of 2008 (Leck & Svensson, 2015; Tjernström et al., 2014). Whereas the CCN concentrations varied by 2 to 3 orders of magnitude over the expedition, occasionally below 1 cm^{-3}, median daily CCN concentrations at 0.2% water vapor supersaturation (SS) were

Writing - Original Draft: Sigurd Christiansen, Luisa Ickes, Ines Bulatovic, Caroline Leck, Elena Gorokhova, Matthew E. Salter, Annica M. L. Ekman, Merete Bilde
Formal Analysis: Sigurd Christiansen, Luisa Ickes, Ines Bulatovic, Caroline Leck
Investigation: Sigurd Christiansen, Luisa Ickes, Ines Bulatovic, Robert Wagner, Elena Gorokhova, Matthew E. Salter, Annica M. L. Ekman, Merete Bilde
Resources: Sigurd Christiansen, Caroline Leck, Benjamin J. Murray, Allan K. Bertram, Elena Gorokhova, Annica M. L. Ekman, Merete Bilde
Supervision: Sigurd Christiansen, Elena Gorokhova, Matthew E. Salter, Annica M. L. Ekman, Merete Bilde
Visualization: Sigurd Christiansen, Luisa Ickes, Ines Bulatovic
Writing - review & editing: Sigurd Christiansen, Luisa Ickes, Ines Bulatovic, Caroline Leck, Benjamin J. Murray, Allan K. Bertram, Robert Wagner, Elena Gorokhova, Matthew E. Salter, Annica M. L. Ekman, Merete Bilde

typically in the range of 15 to 30 cm^{-3} (Leck & Svensson, 2015, Table 1). This agreed with previous observations of CCN concentrations in the area and season (Bigg & Leck, 2001). As a consequence of the low number concentration a small change in the CCN population, either through the number or the chemical composition of the aerosols, may have a strong impact on the lifetime and optical properties of the mixed-phase clouds (Loewe et al., 2017; Prenni et al., 2007; Stevens et al., 2018).

The ability of an aerosol particle to act as a CCN is determined by its size, chemical composition (Köhler, 1936), surface tension (Ovadnevaite et al., 2017), phase (Renbaum-Wolff et al., 2016), and humidity history (Bilde & Svenningsson, 2004; Dusek et al., 2006). The hygroscopicity parameter κ (Petters & Kreidenweis, 2007) is a convenient parameter used to describe the hygroscopic properties of particles even if information about their chemical composition is absent. The κ value can be obtained from experimental data and can be used to describe the CCN activity of aerosol particles in models simulating aerosol-cloud interactions. Atmospherically relevant κ values range from $\kappa = 0$ for insoluble particles to $\kappa = 1.28$ for NaCl (Seinfeld & Pandis, 2016).

As mentioned above measurements of CCN activity directly in the Arctic are few, complicated by the very low particle number concentrations, but in general point toward CCN activities over a wide range of κ values from ~0.1 to ~0.7 (Herenz et al., 2018; Jung et al., 2018, Lange et al., 2018, 2019; Martin et al., 2011; Silvergren et al., 2014; Zábori et al., 2015). These results likely reflect aerosols coming from a wide range of sources including new particle formation (Dall'Osto et al., 2017; Jung et al., 2018), Arctic Haze (Jung et al., 2018; Lange et al., 2018), to some extent sea spray (Lange et al., 2018), frost flowers (Xu et al., 2013), and organic aerosols of biogenic origin including the sea surface microlayer (Lange et al., 2018; Leck & Bigg, 2005a; Orellana et al., 2011).

The current work focuses on CCN activity of SSA and their role for high Arctic clouds and is motivated by the dominance of marine aerosol during both summer (Bigg & Leck, 2008; Leck & Bigg, 2005a) and wintertime (Kirpes et al., 2018, 2019) at coastal and high Arctic sites as well as by the increasing potential for SSA to play a role in Arctic environments and affect cloud properties as a consequence of the rapid decrease in sea ice cover (Struthers et al., 2011).

SSA are formed when air bubbles burst at the sea surface as a part of wave-breaking processes (Lewis & Schwartz, 2004). Chemically, SSA represents a complex mixture of salts and organic constituents (Quinn et al., 2015). The ocean surface is covered by a thin film, the so-called sea surface microlayer (SML), with chemicophysical properties and microbial life different from the bulk water below (Engel et al., 2017; Wurl et al., 2011). Studies of the SML in high Arctic areas has characterized the particulate content (Bigg et al., 2004) and the SML has been shown to contain marine biogenic polymer gels that were also present in aerosol particles, cloud, and fog water (Leck & Bigg, 2005a; Orellana et al., 2011). Further knowledge about the role of the SML for sea-air exchange processes is needed and particular interest centers around the impact of the sea surface microlayer on SSA properties and cloud forming potential (Abbatt et al., 2019; Bigg & Leck, 2008; Gao et al., 2012).

Several laboratory and field studies have addressed CCN activity of SSA using plunging jets or frits to simulate oceanic air entrainment and using NaCl or artificial sea salt mixtures as proxies for the inorganic component of SSA (Collins et al., 2013, 2016; King et al., 2012; Moore et al., 2011). Addition of surfactants to NaCl solution (Prisle et al., 2010) or artificial seawater (King et al., 2012) did not change CCN properties. Even direct coating of sea salt particles with surfactants did not change CCN properties unless very thick (25–29 nm) coatings were applied (Forestieri et al., 2018; Nguyen et al., 2017). Fuentes et al. (2011) and Wex et al. (2010) showed that the effect of phytoplankton exudates addition to inorganic seawater proxy solutions is small (<5–24% and <10%, respectively). SSA generated from seawater from the Bay of Aarhus showed CCN activity similar to inorganic sea salt and was invariant to spiking with SML (Rasmussen et al., 2017). Recent work also demonstrates that CCN activity of SSA generated from seawater using an over-the-side bubbling system is only slightly lower than that of NaCl (Bates et al., 2020).

To our knowledge, no studies have investigated the CCN activity of SML samples collected in the high Arctic or Arctic in general and only one study has addressed CCN activity of exudates from sea ice diatoms (Wex et al., 2010) that are relevant in the Arctic region. Furthermore, modelling studies have shown that high Arctic mixed-phase clouds are often in a CCN-limited regime, that is, that a relatively small change in the

CCN population can result in cloud dissipation (Loewe et al., 2017; Stevens et al., 2018). However, these past studies focused on a change in the number of available aerosols and not the properties of the aerosols.

The current study was performed to address and provide information relevant to the question if and to what extent an organic component of Arctic SSA from sea surface microlayer influences its CCN activity and how that further changes the properties of a typical mixed-phase cloud in the high Arctic. In the first part of the study, we make a comprehensive experimental evaluation of the CCN activity of three types of aerosol particles of increasing complexity: (1) Sea salt aerosols made from artificial seawater, (2) aerosol particles generated from artificial seawater spiked with diatom species cultured in the laboratory (*Melosira arctica*, the most abundant phytoplankton in the Arctic region, and *Skeletonema marinoi*, a diatom typical of temperate regions), and (3) aerosol particles made from samples of SML collected during field campaigns in the North Atlantic and Arctic Ocean. In the second part of the study, we use large-eddy simulation (LES) to evaluate the roles of hygroscopicity and particle size in governing mixed-phase cloud properties, here characterized by the model domain-averaged liquid water path (LWP) and ice water path (IWP). We will simulate the same case as in Stevens et al. (2018) and Loewe et al. (2017) and examine if the properties and size of the CCN may be equally important for the cloud properties as the number of CCN.

2. Materials and Methods

The experiments described herein took place as part of a larger laboratory campaign (Ickes et al., 2020), which was conducted at the Aerosol Interaction and Dynamics in the Atmosphere (AIDA) aerosol and cloud chamber (Möhler et al., 2003, 2008; Wagner et al., 2006, 2012). The same set of samples used for the ice nucleation studies described by Ickes et al. (2020) were used for this work on CCN properties.

2.1. Samples and Chemicals

Two types of organic containing sample were studied: laboratory grown algal cultures and ambient SML samples. For more explicit details on the samples and sample treatment we refer the reader to the campaign overview paper and references therein (Ickes et al., 2020). A short description is given below.

The two laboratory grown diatom species were *S. marinoi* and *M. arctica*. *S. marinoi* is very common, especially in temperate coastal regions during the spring bloom (Borkman & Smayda, 2009; Kooistra et al., 2008). It was grown under three experimental conditions to test the potential effect of different growth rates and cell carbon content on the cloud forming ability of the sample; nutrient-replete conditions (SM100; high growth, high nutrient content of cells), 60% nutrient saturation (SM60; high growth but low-nutrient content), and low-nutrient treatment (SM10; low growth, low-nutrient content). The other culture was *M. arctica*, which is the most productive algae in the Arctic Ocean (Booth & Horner, 1997). Furthermore, particles collected in cloud water in the high Arctic could originate from the *M. arctica* community in the surface microlayer (Orellana et al., 2011). This culture was grown with replete nutrient supply at 6 PSU (practical salinity unit), 5°C, and is referred to as MA100.

SML samples were obtained from two different research expeditions in the Arctic region, NETCARE (Irish et al., 2019) and ASCOS (Gao et al., 2012). The samples from NETCARE were frozen following collection and used without treatment. In this work we use only one sample from the ASCOS expedition (ASCOS 5 kDa to 0.22 μm). Following collection and prior to freezing, this SML sample underwent further treatment aimed at removing salts and enriching the sample in high molecular weight dissolved organic matter (HMW-DOM), see Gao et al. (2012) and Ickes et al. (2020) for details.

In addition to the experiments with algal cultures and SML samples, we performed inorganic reference experiments with pure sea salt (SigmaSS, Sigma Aldrich, S9883; 55% Cl, 31% Na, 8% SO_4^{2-}, 4% Mg, 1% K, 1% Ca, <1% other) and NaCl (NaCl, purity >99.9%, PanReac AppliChem, 381659.1211). For these experiments, particles were generated from a 35 g kg^{-1} solution (20 L) of either sea salt (hereafter referred to as SigmaSS) or NaCl. The CCN counter was calibrated using ammonium sulfate ($(NH_4)_2SO_4$, purity > 99.5%, Merck, 1.01411.0250). Water purified using an ultrapure water system (NANOpure Infinity, Verner Reinstwassersysteme, >17.8 MΩ cm) was used in all experiments. The sweep air for the sea spray tank (see next section) was compressed synthetic air supplied from the AIDA facility.

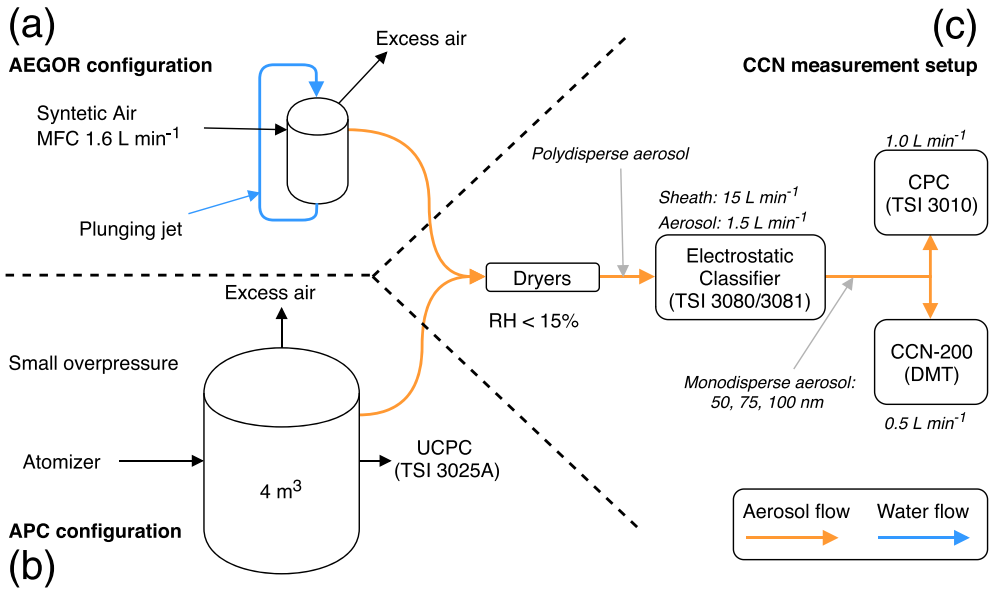

Figure 1. Aerosolization and CCN measurement setup. (a) AEGOR configuration: A plunging jet entrains air and through bubble bursting aerosols are emitted to the headspace. A small overflow of clean air is added and aerosols are directed to the CCN measurement setup. (b) APC configuration: Samples are atomized into the APC chamber at the AIDA facility. (c) CCN measurement setup: Aerosols are first dried to RH < 15% before they are size selected (100, 75, and 50 nm) and divided between a condensation particle counter and a CCN counter.

2.2. Experimental Aerosol Generation and CCN Setup

Two experimental configurations were used to generate aerosol particles (Figure 1). The primary difference between the two configurations was the aerosolization method: (A) Air entrainment followed by bubble bursting in a portable temperature regulated sea spray simulation tank, AEGOR (described in detail elsewhere; Christiansen et al., 2019). This technique generates aerosol particles using a plunging jet to mimic the process of oceanic wave breaking. (B) Atomization into the 3.7 m^3 Aerosol Preparation and Characterization (APC) chamber. The APC chamber, made of stainless steel, belongs to the AIDA facility and was used as an aerosol reservoir (Möhler et al., 2008). In the AEGOR configuration (A), SML samples were diluted with 20 L of sea salt solution, while in the atomizer system (B) SML samples were used undiluted. We applied the atomizer (B) in addition to AEGOR for two main reasons: The ambient SML samples were available in quite small quantities (of the order of milliliters) and given the large volume of AEGOR (20 L) an atomizer was needed to generate aerosols directly from these samples. The atomizer generates higher number concentrations of aerosols than AEGOR from the same solution. Such high number concentrations were needed in some experiments (Ickes et al., 2020), where an additional suite of instruments were used to probe IN properties of the generated aerosols.

Figure 1a shows the AEGOR configuration. SSA were generated from bubble bursting in AEGOR using the plunging jet. The flow rate of the jet was set to 5 L min^{-1} with a nozzle diameter of 4 mm. AEGOR contained 20 L of SigmaSS solution and the water temperature was set to 20°C. For illustration the aerosol particle number size distribution measured in the sea spray tank in Exp. 14 (Table 1) is shown in Figure S1 in the supporting information. An air flow of 1.6 L min^{-1} (excess) was added to the headspace, and 1.5 L min^{-1} of polydisperse aerosol were drawn into the CCN measurement setup. The 20 L inorganic SigmaSS solution was spiked with three different algal cultures (406 mL SM100, 849 mL SM10, and 893 mL MA100).

The APC configuration is shown in Figure 1b. Prior to aerosol injection, the APC chamber was evacuated to a pressure below 1 hPa and filled with particle-free synthetic air. A compressed-air atomizer (1.5 bar) (TSI, Model 3076) was used to aerosolize the undiluted solutions of the algal cultures and SML samples. The generated aerosol particles were injected into the APC chamber with a flow of 3 L min^{-1}. It took 15–30 s to fill the APC chamber to 60.000–100.000 particles per cubic meter. After filling, the atomizer was decoupled and aerosol particles were drawn into the CCN counter from the APC chamber. As the ambient SML samples

Table 1
Overview of Experiments and Obtained CCN Results

				Type	SS_c (%)			κ		
Nr.	Date	Sample	Setup	D_p (nm) →	100	75	50	100	75	50
1	06-02-17	SigmaSS	A	sea salt	0.114	0.177	0.347	1.05	1.04	0.91
2	06-02-17	AS	D	calibration						
3	08-02-17	SM100	A	culture	0.115	0.169	0.322	1.04	1.14	1.06
4	13-02-17	STN2	B	SML	0.115	0.170	0.323	1.04	1.13	1.06
5	14-02-17	STN3	B	SML	0.110	0.169	0.326	1.13	1.13	1.03
6	15-02-17	STN7	B	SML	0.109	0.169	0.324	1.16	1.14	1.05
7	16-02-17	SM10	B	culture	0.109	0.170	0.327	1.15	1.13	1.03
8	16-02-17	SigmaSS	A	sea salt	0.119	0.179	0.358	0.98	1.01	0.86
9	17-02-17	SM10	A	culture	0.110	0.173	0.334	1.13	1.09	0.98
10	17-02-17	SigmaSS	B	sea salt	0.118	0.173	0.324	0.99	1.09	1.05
11	18-02-17	AS	D	calibration						
12	20-02-17	SM100	B	culture	0.115	0.174	0.327	1.04	1.08	1.03
13	20-02-17	SM60	B	culture	0.120	0.174	0.329	0.96	1.08	1.01
14	22-02-17	SigmaSS	A	sea salt	0.112	0.172	0.337	1.08	1.10	0.97
15	22-02-17	MA100	B	culture	0.123	0.182	0.342	0.91	0.98	0.94
16	23-02-17	MA100	A	culture	0.114	0.174	0.335	1.06	1.08	0.98
17	24-02-17	NaCl	B	NaCl	0.111	0.171	0.319	1.11	1.12	1.08
18	24-02-17	ASCOS	B	SML	0.124	0.186	0.360	0.89	0.94	0.85

Note. SigmaSS: Sigma Aldrich sea salts, AS: ammonium sulfate, SM100: high nutrient *S. marinoi*, SM60: 60% nutrient *S. marinoi*, SM10: low-nutrient *S. marinoi*, MA100: *M. arctica*, STN2, STN3, STN7: SML samples from NETCARE (Irish et al., 2019), and ASCOS (HMW-DOM, Gao et al., 2012). The setup column refers to the aerosolization configuration A (AEGOR, plunging jet) and B (atomizer) in Figure 1 and D (calibration) in Figure S2. SS_c is the critical supersaturation at a selected dry mobility diameter, D_p. The uncertainty of SS_c is estimated to be ±0.007% (Harris, 2016). κ is the CCN-derived hygroscopicity parameter. Dates are formatted as DD-MM-YY.

were available in much smaller quantities (volumes) compared to the algal cultures, they were only probed with the atomizer using the APC as a reservoir.

Figure 1c shows the CCN measurement part of the setup. All aerosol particles were dried prior to measurement using silica diffusion dryers to a relative humidity below 15%. The electrostatic classifier was set to size particles at 50, 75, and 100 nm, respectively, and consisted of a Krypton-85 source neutralizer (TSI, 3077 series) and a differential mobility analyzer (TSI, DMA 3081). An impactor (TSI, 0.071 cm) was installed in front of the DMA and the sheath-to-sample flow ratio set to 15:1.5 (gives a cut-point diameter, $D_{50} = 397$ nm, assuming sea salt density is 2.01 g cm^{-3}; Zieger et al., 2017). After size selection, the flow of particles was split between a CCN counter (Droplet Measurement Technologies, CCN-200, 0.5 L min^{-1}) and a condensation particle counter (CPC, TSI 3010, 1 L min^{-1}) to simultaneously measure CCN and total particle number concentrations (condensation nuclei, CN). The CCN counter was set to scan stepwise over a relevant (based on artificial sea salt experiments) range of supersaturation (9–10 steps) with a time interval of 5 min at each supersaturation. The supersaturation of the CCN counter was calibrated using atomized ammonium sulfate according to Rose et al. (2008). Figure S2 illustrates the calibration setup (referred to as "D" in Table 1). Theoretical supersaturations were calculated from the dry particle diameter, with the water activity calculated using the E-AIM (Extended-Aerosol Inorganics Model, https://www.aim.env.uea.ac.uk/aim/aim.php). In the data analysis the first 2 min at each supersaturation were omitted to ensure that temperatures in the column had stabilized. The per second data was averaged on a per minute basis, the activation ratio (CCN/CN) calculated and plotted against the supersaturation to give an activation curve. Critical supersaturations SS_c (the ratio at which 50% of the particles are activated, accounting for multiple charged particles) were obtained based on a sigmoidal fit following Rose et al. (2008). For further details see supplementary material (Figures S2–S4).

2.3. The κ-Köhler Modeling

We model cloud droplet formation using Köhler theory, which provides a relation between droplet diameter (D_p), bulk droplet water activity (a_w), and water vapor saturation ratio (S) (Köhler, 1936):

$$S = a_w \exp\left(\frac{4\sigma_{s/a}M_w}{RT\rho_w D_p}\right) \tag{1}$$

where $\sigma_{s/a}$ is the solution/air surface tension, M_w is the molecular weight of water, ρ_w is the density of water, R is the ideal gas constant, and T is the temperature. The critical supersaturation (SS_c) is the water vapor saturation ratio needed for the droplet to grow only limited by diffusion of water to the droplet surface.

Accounting for nonideality is difficult when the exact chemical composition of the growing droplet is unknown. Petters and Kreidenweis (2007) suggested the following parameterization of the water activity term using the hygroscopicity parameter (κ).

$$\frac{1}{a_w} = 1 + \kappa\frac{V_s}{V_w} \tag{2}$$

where V_s is the dry volume of solute in the droplet and V_w is the volume of water in the droplet. Using this parameterization, the following version of the Köhler equation can be obtained (Petters & Kreidenweis, 2007):

$$S(D_p) = \frac{D_p^3 - D_{p,dry}^3}{D_p^3 - D_{p,dry}^3(1-\kappa)} \exp\left(\frac{4\sigma_{s/a}M_w}{RT\rho_w D_p}\right) \tag{3}$$

Equation 3 was used to derive κ values based on experimentally determined SS_c at specific dry particle diameters ($D_{p,dry}$). $\sigma_{s/a}$ was assumed to be similar to that of water (72 mN m^{-1}) and ρ_w was assumed to be 997 kg m^{-3} (T = 298 K) at all droplet sizes.

2.4. Large-eddy Simulation

2.4.1. Model Description

LES were performed with the *MI*SU (Department of Meteorology, Stockholm University)—*MI*T (Massachusetts Institute of Technology) *C*loud and *A*erosol model (MIMICA). The model solves the equations for a nonhydrostatic, anelastic atmospheric system. A detailed description, together with an evaluation of the model against two well-documented cloud cases, can be found in Savre et al. (2014). Here, the cloud microphysics component of the model is briefly summarized. MIMICA employs a two-moment bulk microphysics scheme for predicting the mass mixing ratio and number concentration of five hydrometeor types, that is, cloud droplets, rain drops, ice crystals, snow and graupel. The mass distributions of the hydrometeors have the form of regular gamma functions where a two-moment approach is used also for calculating auto-conversion, accretion and self-collection (Seifert & Beheng, 2001). The supersaturation is modeled using a pseudo-analytic solution following Morrison and Grabowski (2008), which allows integration of condensation/evaporation at the model time step (i.e., no "saturation adjustment" is applied). The cloud droplets are activated from aerosol particles following Khvorostyanov and Curry (2006) based on κ-Köhler theory (Petters & Kreidenweis, 2007). Ice crystal number concentrations are kept quasi-constant in all simulations as in Morrison et al. (2011); that is, the modeled aerosol particles do not act as ice nuclei. Secondary ice production and aggregation of ice particles are omitted. Wet deposition occurs when the hydrometeors fall out of the cloud, where their terminal fall speeds are calculated using simple power laws of the diameter of the particles.

2.4.2. Simulation Setup

The simulations used in this study are based on a mixed-phase stratocumulus cloud observed from 18 UTC 30 August to 12 UTC 31 August 2008 during the ASCOS campaign (Tjernström et al., 2014). The cloud was characterized by a near-constant cloud base and cloud top (500 and 1,000 m, respectively) during this period (Shupe et al., 2013). A thermodynamic sounding from approximately 06 UTC 31 August 2008 is used to initialize the simulations. All simulations are initialized with a cloud layer present, that is, with a prescribed cloud water mixing ratio profile derived from observations. As such, aerosol activation is not needed for the initial formation of the cloud, only to sustain the cloud. The simulation period is 12 hr where the first 2 hr are considered as a spin-up period of the model.

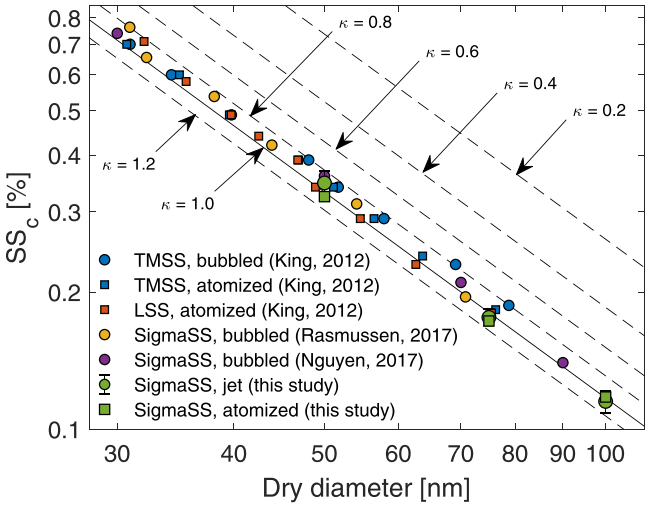

Figure 2. Critical supersaturation, SS_c, as a function of dry mobility diameter for inorganic salt solutions, that is, TMSS (Tropic Marin Sea Salt), LSS (Laboratory Sea Salt), and SigmaSS (Sigma Aldrich Sea Salt) from this work and literature. Circles represent aerosolization by bubble bursting and squares represent atomization; κ lines are shown for a value of 1.2, 1.0, 0.8, 0.6, 0.4, and 0.2.

The 3-D model domain is defined by $96 \times 96 \times 128$ grid points ($6 \times 6 \times 1.7\,km^3$) with a fixed 62.5 m distance between grids in the horizontal direction and a variable grid spacing in the vertical. The smallest grid cells in the vertical direction (7.5 m) are at the surface and in the cloud layer. A model time step of 2 s or shorter is applied depending on a numerical stability criterion. Surface sensible and latent heat fluxes are turned off since the observed turbulent fluxes were very small (cf. Tjernström et al., 2014). The surface temperature is prescribed to 269.8 K, and the surface pressure is 1,026.3 hPa. The large-scale divergence rate is set to $1.5 \times 10^{-6}\,s^{-1}$ over the whole model domain. The prescribed surface albedo value is 0.844. A radiation solver is dynamically coupled to the model (Fu & Liou, 1993).

The Aitken and accumulation aerosol populations are represented by log-normal modes, where the distribution parameters for each mode are based on the ASCOS measurements (cf. Igel et al., 2017). Modal diameters of 32 and 93 nm and standard deviations of 1.1 and 1.5 are used for the Aitken and accumulation modes, respectively. The aerosol concentrations are assumed to be constant with height and prescribed to values that are in line with the observations. To test the sensitivity of the simulated cloud properties to particle hygroscopicity and size, a total of four sets of simulations were conducted. Two of them only consider Aitken mode aerosols with initial aerosol concentrations of 15 and $30\,cm^{-3}$ (referred to as Aitken_15 and Aitken_30, respectively). The other two sets only consider accumulation mode aerosols with the same two number concentrations (referred to as acc_15 and acc_30, respectively). For the sensitivity simulations, a range of hygroscopicity values that cover those reported in the literature (cf. section 1), from 0.2 (i.e., close to hydrophobic) to 1.2 (i.e., highly hygroscopic), are used to explore the importance of κ. Each simulation set thus contains six cases with different κ values (0.2; 0.4; 0.6; 0.8; 1.0; 1.2). A quasi-constant concentration of ice crystals is prescribed to $0.2\,L^{-1}$ (Loewe et al., 2017) and is the same in all simulations. Note that the simulated cloud microphysics and cloud characteristics are most likely more sensitive to other microphysical and meteorological parameters than the κ value, for example, the temperature of the cloud and the ice crystal concentration. However, we focus here on the sensitivity to hygroscopicity in accordance with the experimental part of the study.

3. Results and Discussion

3.1. CCN Activity of Sea Salt Aerosols

Table 1 provides an overview of all of the experiments performed in this study along with experimentally determined critical supersaturations (SS_c) and derived κ values. We first consider the baseline experiments of CCN activity of particles generated from an artificial sea salt solution. Such experiments were conducted regularly throughout the campaign and demonstrated reproduceability (Figure S3). The CCN activity of SigmaSS particles in the diameter size range 50–100 nm is in broad agreement with previous results (King et al., 2012; Nguyen et al., 2017; Rasmussen et al., 2017) (see Figure 2) with CCN-derived κ values in the range 0.86–1.08 with an average κ value of 1.01 ± 0.07 (based on Table 1). The study by Rasmussen et al. (2017) points out that several salts present in sea salt form hydrates, which keep their water during drying at ambient temperatures. As such, hydrate water can account for a significant volume fraction of dried sea salt. We cannot exclude that different brands of artificial sea salt may contain slightly different relative amounts of hydrate forming salts, in particular, $MgCl_2$ and $CaCl_2$. Furthermore, some salts may exist in several hydration states (Kelly & Wexler, 2005) and thus exact amount of hydrate bound water in dried sea salt particles may vary depending on drying method. In combination with potential differences in particle shapes this may explain the slight differences between SS_c for the same dried particles size in different studies in Figure 2. A single experiment was performed on atomized NaCl particles yielding a κ value of 1.1 ± 0.1 slightly lower than the theoretical value of 1.28 (Topping et al., 2016). For comparison, Zieger et al. (2017) suggest a κ value of 1.1 from hygroscopic growth measurements at 90% RH, which is slightly higher than the CCN-derived value. Similar behavior has been observed for other compounds (Petters & Kreidenweis, 2007).

3.2. CCN Activity of Algal Cultures and Arctic SML

As described in section 2.2 two types of experiments were performed using laboratory grown algae cultures: In the first type, algae cultures were added to an artificial sea salt solution in AEGOR and SSA was generated

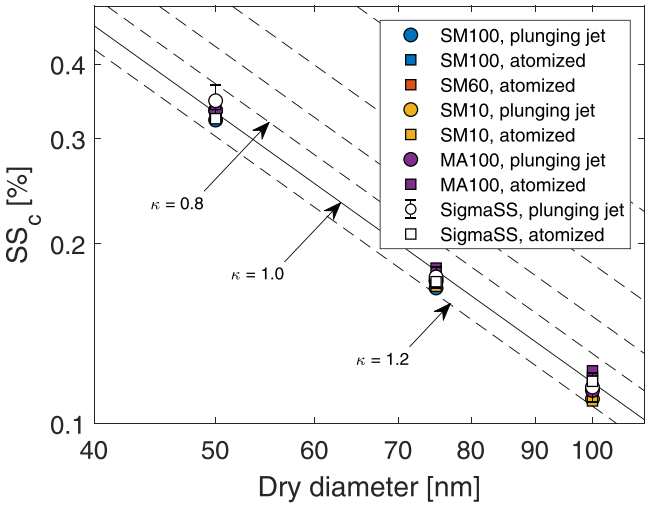

Figure 3. Critical supersaturation, SS_c, as a function of dry mobility diameter for different algae cultures. The plunging jet (circle symbol) and atomized (square symbol) results are shown for different cultures. The error bars on SigmaSS indicate ±1 standard deviation based on three replicate experiments.

using bubble bursting (plunging jet). In the second type of experiments particles were generated by atomization of the undiluted algae cultures. Figure 3 shows that within the experimental uncertainties of this work all particles have CCN behavior similar to that of sea salt particles. The only exception is for a few of the 50 nm experiments, that is, SM100 and SM10 in AEGOR, and MA100 when atomized, see Figures S5 and S6. For 50 nm (diameter) particles generated by spiked seawater (SM100 and SM10) in AEGOR a slight (~7%) increase in CCN activity compared to sea salt is observed, while for the atomized MA100 culture a slight (~6%) decrease in CCN activity is observed. The fact that the atomized MA100 increased the SS_c is likely related to the fact that the salinity of this sample was only 6 PSU (Ickes et al., 2020), compared to ~35 PSU when spiked in SigmaSS. Overall the agreement with the CCN activity (SS_c) of sea salt is always within 10%. For comparison, Fuentes et al. (2011) observed agreement (within 5–24%) between the CCN activity of particles generated from artificial seawater spiked with algal exudates and particles generated from artificial seawater with the largest deviation for the smallest particles.

Figure 4 shows the CCN activity of aerosolized SML samples from different locations in the Arctic. It is evident that for these field samples the CCN activity is also similar to that of sea salt within the measurement uncertainties. Even for the ASCOS samples that were enriched in HMW-DOM due to treatment (see section 2.1) only the small particles (50 nm) show a slight (~11%) deviation from the SS_c of sea salt. The average κ value obtained from all experiments (SML and cultures) conducted herein is 1.06 ± 0.07. This is slightly higher, but within uncertainties similar to the κ value of inorganic sea salt (1.01 ± 0.07).

Our observations are consistent with those of Rasmussen et al. (2017), where seawater samples and seawater samples spiked with sea surface microlayer from the bay of Aarhus show CCN activity similar to that of sea salt (Figure 4, "Aarhus"). In addition, recent field (Bates et al., 2020) and laboratory (Collins et al., 2016) studies conclude that plankton blooms have little effect on the CCN activity of primary SSA. Our work in combination with the preceding studies of Rasmussen et al. (2017), Collins et al. (2016), and Bates et al. (2020) suggests that the CCN activity of particles generated from seawater and SML samples is largely unaffected by even significant amounts of organic substances in the water from which they originate.

There could be several reasons for the observed behavior. As shown and discussed by Bilde and Svenningsson (2004), a soluble salt will dominate CCN activity, despite the presence of soluble or slightly soluble organics, even if the salt is only present in trace (of the order of a few percent) amounts. Nguyen et al. (2017) recently showed that even large volume fractions (25% to 96%) of low soluble surface active material in the form of saturated or unsaturated fatty acids did not hinder the water uptake of laboratory generated SSA. The study by Forestieri et al. (2018) supported this finding.

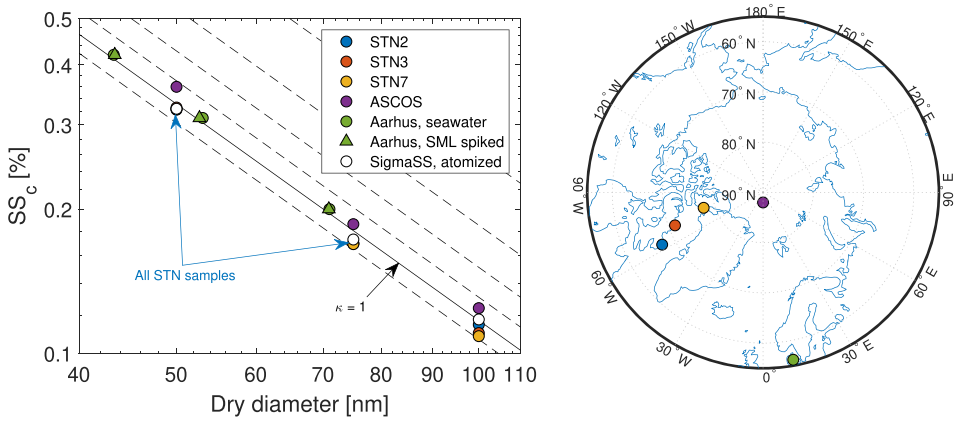

Figure 4. (left) Critical supersaturation as a function of dry mobility diameter in of four SML samples. For comparison inorganic sea salt and results from Rasmussen et al. (2017) are added. (right) Map of sampling locations.

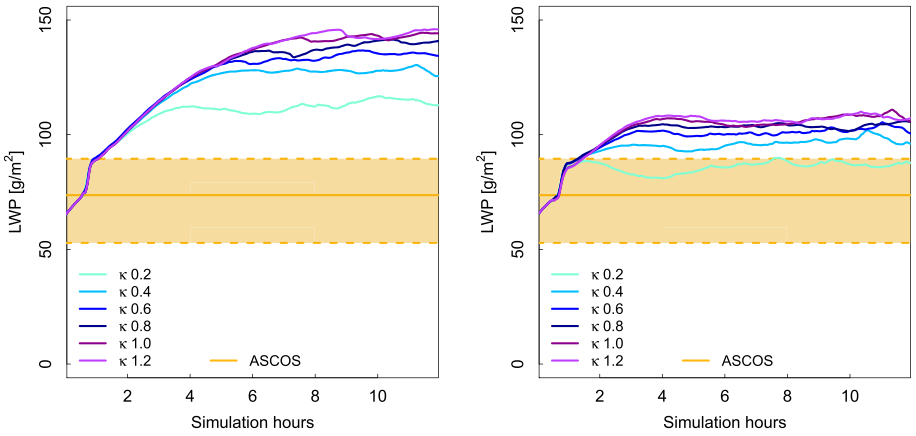

Figure 5. Time evolution of the simulated domain-averaged liquid water path for the simulation set acc_30 (left) and acc_15 (right) for a range of different κ values. "acc" refers to accumulation mode and 30 to the particle concentration, see section 2.4.2 for notation. The line denoted ASCOS refers to the retrieved LWP from microwave radiometer measurements (median over the observation period; the corresponding dashed lines are the 25th/75th percentiles). Note that the first 2 hr are considered as a spin-up period of the model.

While SSA generated in the laboratory from bubble bursting appear to have a consistent κ value of ~1, irrespective of the composition of the seawater they originate from and how bubbles are generated, ambient marine boundary layer aerosols, including those found in the high Arctic, are consistently less hygroscopic in comparison (κ in the range 0.1–0.7 as discussed in section 1). The main reason for this discrepancy is likely that most of the available ambient CCN measurements provide ensemble properties of aerosols from several sources for example Arctic Haze (Jung et al., 2018; Schmale et al., 2018) and biogenic (Dall'Osto et al., 2017; Lange et al., 2019) sources. This is further supported by the recent work of Bates et al. (2020) showing that SSA generated in situ over the North Atlantic Ocean showed CCN activity similar to salt independent of the different plankton bloom stages. Furthermore, the laboratory systems generate fresh SSA, while in several cases the field studies probe aerosols generated through other mechanisms such as secondary processes and/or aerosols that have been transported over long distances and thus have undergone chemical and physical changes due to aging processes (Leck & Bigg, 2005b) (e.g., via condensation of vapors or chemical reactions at the surface and inside the aerosol). To span the full range of observed κ values in the field and the κ values found in the laboratory and in situ for fresh SSA in the following, we test the impact of varying hygroscopicity over a range of hygroscopicities that encapsulate both field and laboratory observations on a typical Arctic mixed-phase cloud.

3.3. Impact of κ Value and Aerosol Size on Simulated Cloud Properties

In the following section, we investigate the impact of the hygroscopicity (κ value) and the size of aerosol particles on a simulated quasi-steady mixed-phase low-level cloud layer, typical for the summertime high Arctic. This cloud is in general believed to be in "the CCN-limited regime"; that is, it should be sensitive to the number of available CCN (Stevens et al., 2018). Simulation sets were conducted for different aerosol sizes and for different κ values ranging from close to hydrophobic ($\kappa = 0.2$) to very hygroscopic ($\kappa = 1.2$).

3.3.1. Accumulation Mode

In the first set of simulations for the accumulation mode (30 cm^{-3}, see section 2.4.2 for notation), the κ value has in general a minor influence on the simulated LWP and IWP (acc_30; Figure 5, left panel). It is only for very low κ values ($\kappa < 0.4$) that the hygroscopicity of aerosols substantially impacts the cloud water content (15% decrease in average LWP over the whole simulation period for the simulation with $\kappa = 0.2$ compared to the simulation with $\kappa = 1.2$). For aerosols with a larger κ value, there is almost no influence of the aerosol hygroscopicity on the total cloud water content (maximum 4% of change in average LWP over the whole simulation period). This result implies that all accumulation mode aerosols with a κ larger than 0.4 are efficient as CCN. It also shows that the cloud is sustained for all of the simulated cases, even when the aerosols are close to hydrophobic ($\kappa = 0.2$). The LWP is lower for the case with $\kappa = 0.2$, but the cloud layer is still stable.

The amount of cloud ice is not affected substantially by the different κ values, differences are less than 13% when comparing the average IWP over the whole simulation period (not shown). The sensitivity to κ is also similar when using a lower accumulation mode aerosol number concentration (acc_15; Figure 5, right panel); we obtain a consistent threshold κ value of 0.4. Summarizing, the cloud microphysical properties

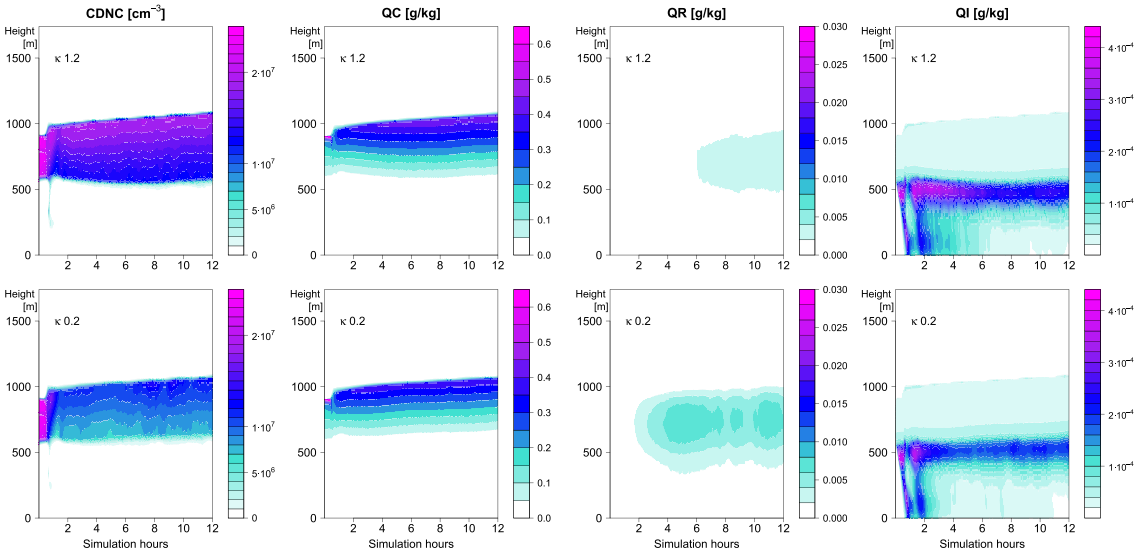

Figure 6. Evolution of horizontally averaged cloud microphysical parameters (cloud droplet number concentration (CDNC), cloud water (QC), rain water (QR), and cloud ice (QI)) simulated for hygroscopic aerosols with a maximum κ of 1.2 (upper row) and hydrophobic aerosols with a minimum κ value of 0.2 (lower row). Both simulations are from the set acc_30.

(e.g., simulated LWP and IWP) do not depend strongly on the accumulation mode hygroscopicity. This is most likely because these particles are large enough in size to be CCN-active regardless of the κ value. However, it is worth noting that the conclusions are drawn for one specific case and that they may be dependent on the model choice as different models produce different amounts of cloud water for the same case (Stevens et al., 2018).

To study the impact of aerosol hygroscopicity on the evolution of the cloud in more detail, the cloud droplet number concentration (CDNC), mixing ratios for cloud water (QC), rain (QR), and ice (QI) as a function of height for two of the simulations in the set acc_30 are displayed in Figure 6. The upper row of Figure 6 shows results from the simulation with the maximum κ value ($\kappa = 1.2$) while the lower row shows results from the simulation with the minimum κ value tested ($\kappa = 0.2$). In both simulations there is a persistent mixed-phase cloud at a height from approximately 400 to 1,000 m with ice precipitation falling out of the cloud. However, the microphysical structure of the cloud is different depending on the κ value. A high κ value leads to enhanced activation of aerosols and thus more CDNC compared to the simulation with the minimum κ value. With a lower κ, the supersaturation spectrum shifts to higher values compared to when a maximum κ is used and the less hygroscopic aerosols are eventually also activated (Figure 7; cf. also Chandrakar et al., 2017). The droplets in the simulation with the minimum κ value are larger compared to the case with very hygroscopic aerosols and the precipitation (QR) is consequently stronger. There is also

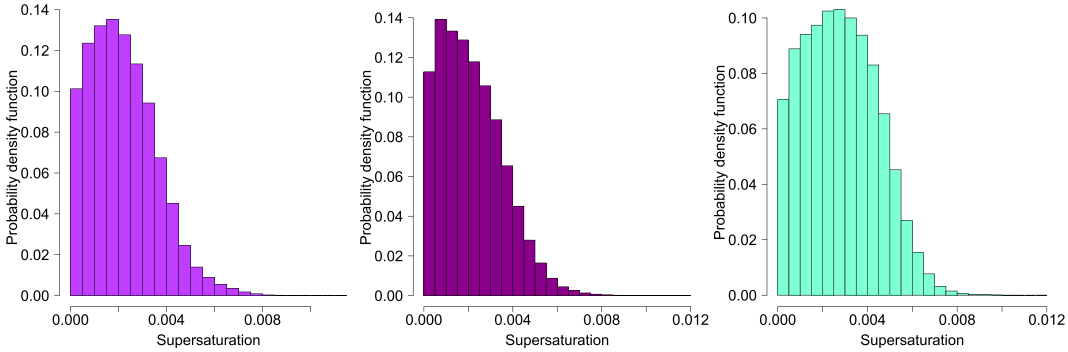

Figure 7. Simulated supersaturation at 4 h of simulation for three cases from the acc_30 set: The simulation assuming a maximum κ (1.2) is shown on the left, κ=1 (i.e., the κ that agrees best with observations) is on the middle, and the one with minimum κ (0.2) is shown on the right.

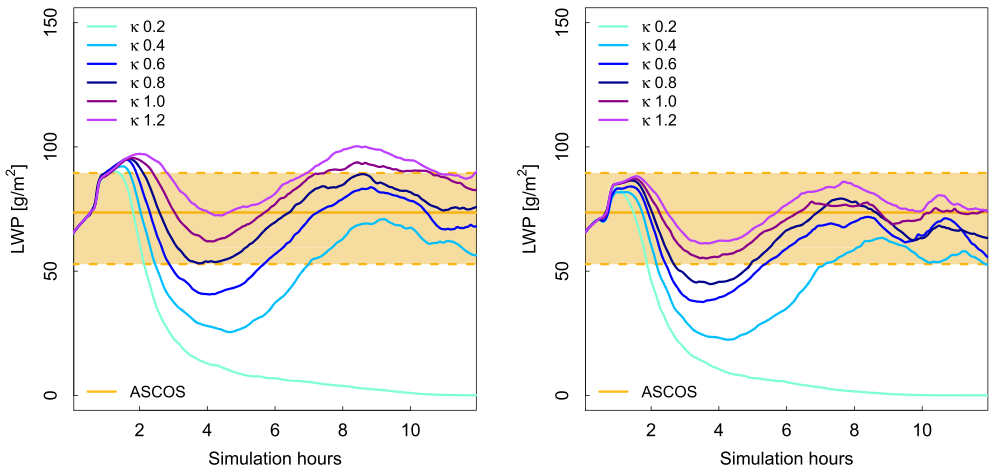

Figure 8. Time evolution of the simulated domain-averaged liquid water path for the simulation set Aitken_30 (left) and Aitken_15 (right) for a range of different κ values. The line denoted ASCOS refers to the retrieved LWP from microwave radiometer measurements (median over the observation period; the corresponding dashed lines are the 25th/75th percentiles). Note that the first 2 hr are considered as a spin-up period of the model.

more cloud ice in the simulation with more cloud droplets (maximum κ). In the simulation with lower κ value, cloud droplets are lost due to precipitation and less droplets are available for freezing.

3.3.2. Aitken Mode

Here we examine the impact of a change in aerosol size; that is, we evaluate and compare the simulation set Aitken_30 with acc_30. Note that for simplicity, we denote both size distributions according to their median diameter size. However, in both cases, aerosols within the whole range of the log-normal size distribution can affect the cloud, that is, aerosols that are larger/smaller than the median diameter are present and can activate as cloud droplets. Using the size distribution of the smaller particles (Aitken_30), the κ value has a relatively strong influence on the simulated liquid water path (Figure 8, left panel). When the aerosols are smaller, the aerosol hygroscopicity becomes more important for activation. Still, in nearly all simulations, the Aitken mode aerosols can sustain a stable mixed-phase cloud. It is only for the lowest κ value ($\kappa = 0.2$) that the cloud dissipates. In contrast to the accumulation mode simulations, the cloud water amount clearly depends on the κ value. We can distinguish between two regimes: One regime for κ-value that is greater than or equal to 0.4 and one for κ value less than 0.4. In the first regime, the cloud is persistent during the simulation time and the LWP increases with increasing κ. For a simulation with a κ value below 0.4, no stable cloud is sustained. Due to the low hygroscopicity of particles in this case, the aerosols are not activated and therefore the cloud (which is present initially in the simulation) dissipates quickly. The corresponding simulations with lower aerosol concentrations (Aitken_15; see Figure 8, right panel) show similar results as the simulation set with higher aerosol concentration (Aitken_30). The time evolution of horizontally averaged CDNC, QC, QR, and QI for the simulation in the Aitken_30 set with a maximum κ is shown in Figure 9. One may see that due to the reduced activation of cloud droplets CDNC, QC, and QI are smaller compared to the accumulation mode simulations (Figure 6). That increases fall out of cloud droplets and ice (see QR and QI in Figure 9).

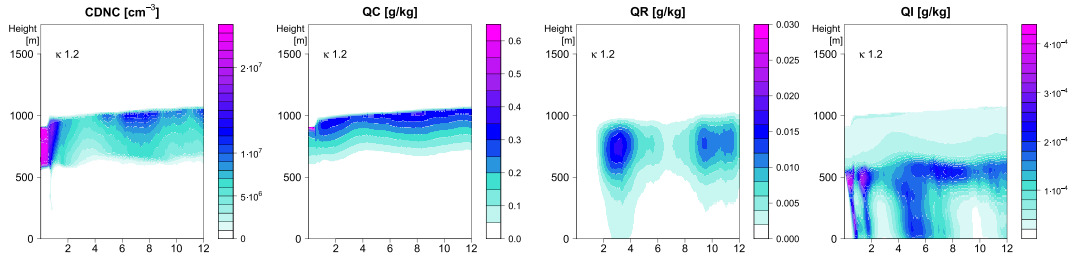

Figure 9. Evolution of horizontally averaged cloud microphysical parameters (cloud droplet number concentration (CDNC), cloud water (QC), rain water (QR), and cloud ice (QI)) simulated for hygroscopic aerosols with a maximum κ of 1.2. The simulation is from the set Aitken_30.

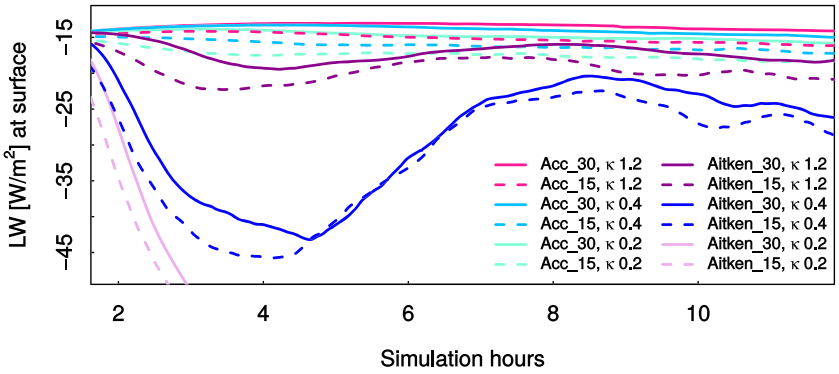

Figure 10. Impact of the different simulations settings (aerosol size, aerosol concentration, and κ value) on the surface longwave (LW) energy budget showing three simulations (maximum, minimum, and threshold κ) from each simulation set (acc_30, acc_15, Aitken_30, and Aitken_15). The radiation is net downwelling at the surface ($LW_{down} - LW_{up}$), that is, a negative value of net LW at the surface means that the net LW radiation is outgoing from the surface.

3.3.3. Surface Energy Budget

A change in cloud microphysical properties induced by a change in aerosol size (accumulation or Aitken), concentration (15 or 30 cm^{-3}) or aerosol hygroscopicity (a range of κ values from 0.2 to 1.2) will also affect the surface energy budget. Since the longwave (LW) radiation is more important than the shortwave radiation at high latitudes, we focus on changes in the net longwave radiation (Figure 10 and Table 2). A higher κ value leads to optically thicker clouds, higher LWP and less outgoing LW radiation (i.e., a less negative value). The LWP is lower and there is more LW cooling if only Aitken mode aerosols are available. In this case the LWP and the radiative properties of the cloud are also sensitive to the aerosol hygroscopicity. A higher number of aerosols leads to higher LWP, optically thicker clouds and less cooling of the surface.

4. Conclusion and Outlook

The CCN-derived hygroscopicity parameter, κ, is found to be ~1.0 for sea salt aerosols generated from artificial seawater consistent with previous studies. SSA generated from artificial seawater spiked with the algal cultures, *S. marinoi*, and the most productive species in the Arctic, *M. arctica*, show CCN activity indistinguishable from inorganic sea salt. The same conclusion applies for particles generated directly from SML

Table 2
Overview of the Mean LWP and Net LW at the Surface for the Simulated Cloud Over the Last Hour of Simulation Time

Sim.	κ	Mean LWP (g m^{-2})	Mean IWP (g m^{-2})	Mean net LW at surface (W m^{-2})	Mean albedo
Acc_30	1.2	145.6	4.8	−14	0.49
Acc_30	1.0	144.1	4.5	−14.1	0.49
Acc_30	0.4	128.1	5.5	−14.8	0.51
Acc_30	0.2	114	4.6	−15.7	0.48
Acc_15	1.2	107.0	4.2	−16.1	0.47
Acc_15	1.0	108.4	5.1	−16.1	0.41
Acc_15	0.4	96.9	4.1	−17.1	0.43
Acc_15	0.2	87.1	3.4	−18.3	0.45
Aitken_30	1.0	84.8	4.3	−18.7	0.4
Aitken_30	0.4	59.5	3.0	−25.3	0.43
Aitken_30	0.2	0.1	1.6	−81.8	0
Aitken_15	1.0	73.6	3.4	−21.3	0.33
Aitken_15	0.4	55.5	2.5	−27.0	0.41
Aitken_15	0.2	0	0.2	−82.0	0

samples from two different research expeditions in the Arctic region. While this work shows that CCN activity is unaffected by the presence of marine organic material, the related work presented in Ickes et al. (2020) on the same samples show a large variability in ice nucleation activity suggesting that the two are decoupled. This reflects the different mechanisms of activation: CCN activation is related to water soluble mass while ice nucleation is related to the presence of specific ice active components with, for example, active sites or ice active proteins (Murray et al., 2012; Holden et al., 2019). In general, the more material that has the potential to nucleate ice that is present in a particle, the greater the probability of nucleating ice. Hence, we might expect SSA with a greater proportion of biogenic organic material, which is known to contain ice nucleating entities (Schnell & Vali, 1975; Wilson et al., 2015), to have a greater probability to nucleate ice. The results in this paper suggest that these organic laden particles can still serve as effective CCN despite the reduced hygroscopic salt content, which means that the ice nucleating entities that they contain can become immersed in cloud droplets and therefore play a role in cloud ice formation.

LES of a typical low-level Arctic mixed-phase cloud case show that hygroscopicity does not have a large influence on the modeled cloud microphysical variables (e.g., LWP and IWP) if the aerosols are of accumulation mode size or larger and if the κ value is larger than 0.4. Below this κ threshold, the LWP and longwave surface heating of the simulated cloud is reduced significantly with decreasing κ. The hygroscopicity of aerosols (reflected by the κ value) becomes more important if the aerosols are small, that is, Aitken mode size. In this case, the simulated LWP (and radiative properties of the cloud) always depend on the hygroscopicity of the aerosols and the cloud can only be sustained if the κ value is 0.4 or higher. Note that the exact values of these κ thresholds may be dependent on the model choice as well as the selected case. Overall, the results from the simulated case combined with the measurements suggest that internal mixing of biogenic organics in SSA has a relatively small influence on the cloud droplet activation process and characteristics of Arctic mixed-phase clouds.

This work contributes for the first time information about the CCN activity of SML samples from the Arctic and even high Arctic and insight into how variability in aerosol hygroscopicity affects Arctic cloud properties. Future work should address broader implications of a potential increase in sea spray formation in the Arctic.

Data Availability Statement

Experimental and model data are available online (https://doi.org/10.5281/zenodo.3932955) (DOI: 10.5281/zenodo.3932954).

References

Abbatt, J. P. D., Richard Leaitch, W., Aliabadi, A. A., Bertram, A. K., Blanchet, J. P., Boivin-Rioux, A., et al. (2019). Overview paper: New insights into aerosol and climate in the Arctic. *Atmospheric Chemistry and Physics*, *19*(4), 2527–2560. https://doi.org/10.5194/acp-19-2527-2019

Bates, T. S., Quinn, P. K., Coffman, D. J., Johnson, J. E., Upchurch, L., Saliba, G., et al. (2020). Variability in marine plankton ecosystems are not observed in freshly emitted sea spray aerosol over the North Atlantic Ocean. *Geophysical Research Letters*, *47*, e2019GL085938. https://doi.org/10.1029/2019GL085938

Bigg, E. K., & Leck, C. (2001). Properties of the aerosol over the central Arctic Ocean. *Journal of Geophysical Research*, *106*(D23), 32,101–32,109. https://doi.org/10.1029/1999JD901136

Bigg, E. K., & Leck, C. (2008). The composition of fragments of bubbles bursting at the ocean surface. *Journal of Geophysical Research*, *113*, D11209. https://doi.org/10.1029/2007JD009078

Bigg, E. K., Leck, C., & Tranvik, L. (2004). Particulates of the surface microlayer of open water in the central Arctic Ocean in summer. *Marine Chemistry*, *91*(1-4), 131–141. https://doi.org/10.1016/j.marchem.2004.06.005

Bilde, M., & Svenningsson, B. (2004). CCN activation of slightly soluble organics: The importance of small amounts of inorganic salt and particle phase. *Tellus, Series B: Chemical and Physical Meteorology*, *56*(2), 128–134. https://doi.org/10.1111/j.1600-0889.2004.00090.x

Blunden, J., & Arndt, D. S. (2019). State of the Climate in 2018. *Bulletin of the American Meteorological Society*, *100*(9), Si–S305. https://doi.org/10.1175/2019BAMSStateoftheClimate.1

Booth, B. C., & Horner, R. A. (1997). Microalgae on the Arctic ocean section, 1994: Species abundance and biomass. *Deep-Sea Research Part II: Topical Studies in Oceanography*, *44*(8), 1607–1622. https://doi.org/10.1016/S0967-0645(97)00057-X

Borkman, D. G., & Smayda, T. (2009). Multidecadal (1959-1997) changes in Skeletonema abundance and seasonal bloom patterns in Narragansett Bay, Rhode Island, USA. *Journal of Sea Research*, *61*(1-2), 84–94. https://doi.org/10.1016/j.seares.2008.10.004

Boucher, O., Randall, D., Artaxo, P., Bretherton, C., Feingold, G., Forster, P., et al. (2013). Clouds and aerosols. *Climate Change 2013: The Physical Science Basis. Contribution of Working Group I to the Fifth Assessment Report of the Intergovernmental Panel on Climate Change*, 571–657. https://doi.org/10.1017/CBO9781107415324.016

Chandrakar, K. K., Cantrell, W., Ciochetto, D., Karki, S., Kinney, G., & Shaw, R. A. (2017). Aerosol removal and cloud collapse accelerated by supersaturation fluctuations in turbulence. *Geophysical Research Letters*, *44*, 4359–4367. https://doi.org/10.1002/2017GL072762

Acknowledgments

This project/work has received funding from the European Union's Horizon 2020 research and innovation program through the EUROCHAMP-2020 Infrastructure Activity under Grant Agreement 730997. We gratefully acknowledge the support by the technical staff of the AIDA facility. L. I. was supported by the Swiss National Science Foundation (Early Postdoc.Mobility). M. E. S. was supported by the Swedish Science Foundation (Vetanskapsrådet) with Grant 2016-05100. The simulations were enabled by resources provided by the Swedish National Infrastructure for Computing (SNIC) at the National Supercomputer Centre (NSC) partially funded by the Swedish Research Council through Grant Agreement 2016-07213. We thank Hamish Struthers at the National Supercomputing Centre at Linköping University for his assistance, which was made possible through application support provided by SNIC. We also thank the Swedish Science Foundation (Vetenskapsrådet), Grant 2015-05318, and the Knut and Alice Wallenberg Foundation, project Arctic Climate Across Scales (ACAS) and the Helmholtz-Gemeinschaft Deutscher Forschungszentren (program "Atmosphere and Climate"). S. C. thanks the Faroese Research Foundation, Grant 0454. B. J. M. thanks the European Research Council (ERC, Marinelce 648661) for a fellowship.

Christiansen, S., Salter, M. E., Gorokhova, E., Nguyen, Q. T., & Bilde, M. (2019). Sea spray aerosol formation: Laboratory results on the role of air entrainment, water temperature, and phytoplankton biomass. *Environmental Science & Technology*, *53*(22), 13,107–13,116. https://doi.org/10.1021/acs.est.9b04078

Collins, D. B., Ault, A. P., Moffet, R. C., Ruppel, M. J., Cuadra-Rodriguez, L. A., Guasco, T. L., et al. (2013). Impact of marine biogeochemistry on the chemical mixing state and cloud forming ability of nascent sea spray aerosol. *Journal of Geophysical Research: Atmospheres*, *118*, 8553–8565. https://doi.org/10.1002/jgrd.50598

Collins, D. B., Bertram, T. H., Sultana, C. M., Lee, C., Axson, J. L., & Prather, K. A. (2016). Phytoplankton blooms weakly influence the cloud forming ability of sea spray aerosol. *Geophysical Research Letters*, *43*, 9975–9983. https://doi.org/10.1002/2016GL069922

Dall'Osto, M., Beddows, D. C. S., Tunved, P., Krejci, R., Ström, J., Hansson, H. C., et al. (2017). Arctic sea ice melt leads to atmospheric new particle formation. *Scientific Reports*, *7*(1), 1–10. https://doi.org/10.1038/s41598-017-03328-1

Dusek, U., Frank, G. P., Hildebrandt, L., Curtius, J., Schneider, J., Walter, S., et al. (2006). Size matters more than chemistry for cloud-nucleating ability of aerosol particles. *Science*, *312*(5778), 1375–1378. https://doi.org/10.1126/science.1125261

Engel, A., Bange, H. W., Cunliffe, M., Burrows, S. M., Friedrichs, G., Galgani, L., et al. (2017). The ocean's vital skin: Toward an integrated understanding of the sea surface microlayer. *Frontiers in Marine Science*, *4*, 165. https://doi.org/10.3389/fmars.2017.00165

Forestieri, S. D., Staudt, S. M., Kuborn, T. M., Faber, K., Ruehl, C. R., Bertram, T. H., & Cappa, C. D. (2018). Establishing the impact of model surfactants on cloud condensation nuclei activity of sea spray aerosol mimics. *Atmospheric Chemistry and Physics*, *18*(15), 10,985–11,005. https://doi.org/10.5194/acp-18-10985-2018

Fu, Q., & Liou, K. N. (1993). Parameterization of the radiative properties of cirrus clouds. *Journal of the Atmospheric Sciences*, *50*(13), 2008–2025. https://doi.org/10.1175/1520-0469(1993)050<2008:POTRPO>2.0.CO;2

Fuentes, E., Coe, H., Green, D., & McFiggans, G. (2011). On the impacts of phytoplankton-derived organic matter on the properties of the primary marine aerosol—Part 2: Composition, hygroscopicity and cloud condensation activity. *Atmospheric Chemistry and Physics*, *11*(6), 2585–2602. https://doi.org/10.5194/acp-10-9295-2010

Gao, Q., Leck, C., Rauschenberg, C., & Matrai, P. A. (2012). On the chemical dynamics of extracellular polysaccharides in the high Arctic surface microlayer. *Ocean Science*, *8*(4), 401–418.

Harris, D. C. (2016). *Quantitative chemical analysis* (ninth).: Macmillan.

Herenz, P., Wex, H., Henning, S., Kristensen, T. B., Rubach, F., Roth, A., et al. (2018). Measurements of aerosol and CCN properties in the Mackenzie River delta (Canadian Arctic) during spring-summer transition in May 2014. *Atmospheric Chemistry and Physics*, *18*(7), 4477–4496. https://doi.org/10.5194/acp-18-4477-2018

Holden, M. A., Whale, T. F., Tarn, M. D., O'Sullivan, D., Walshaw, R. D., Murray, B. J., et al. (2019). High-speed imaging of ice nucleation in water proves the existence of active sites. *Science Advances*, *5*(2), eaav4316. https://doi.org/10.1126/sciadv.aav4316

Ickes, L., Porter, G. C. E., Wagner, R., Adams, M. P., Bierbauer, S., Bertram, A. K., et al. (2020). The ice-nucleating activity of Arctic sea surface microlayer samples and marine algal cultures. *Atmospheric Chemistry and Physics*, *20*(20), 1–28. https://doi.org/10.5194/acp-20-11089-2020

Igel, A. L., Ekman, A. M. L., Leck, C., Tjernström, M., Savre, J., & Sedlar, J. (2017). The free troposphere as a potential source of arctic boundary layer aerosol particles. *Geophysical Research Letters*, *44*, 7053–7060. https://doi.org/10.1002/2017GL073808

Irish, V. E., Hanna, S. J., Xi, Y., Boyer, M., Polishchuk, E., Ahmed, M., et al. (2019). Revisiting properties and concentrations of ice-nucleating particles in the sea surface microlayer and bulk seawater in the Canadian Arctic during summer. *Atmospheric Chemistry and Physics*, *19*(11), 7775–7787. https://doi.org/10.5194/acp-19-7775-2019

Jung, C. H., Yoon, Y. J., Kang, H. J., Gim, Y., Lee, B. Y., Ström, J., et al. (2018). The seasonal characteristics of cloud condensation nuclei (CCN) in the arctic lower troposphere. *Tellus B: Chemical and Physical Meteorology*, *70*(1), 1–13. https://doi.org/10.1080/16000889.2018.1513291

Köhler, H. (1936). The nucleus in and the growth of hygroscopic droplets. *Transactions of the Faraday Society*, *32*(0), 1152–1161. https://doi.org/10.1039/TF9363201152

Kelly, J. T., & Wexler, A. S. (2005). Thermodynamics of carbonates and hydrates related to heterogeneous reactions involving mineral aerosol. *Journal of Geophysical Research*, *110*, D11201. https://doi.org/10.1029/2004JD005583

Khvorostyanov, V. I., & Curry, J. A. (2006). Aerosol size spectra and CCN activity spectra: Reconciling the lognormal, algebraic, and power laws. *Journal of Geophysical Research*, *111*, D12202. https://doi.org/10.1029/2005JD006532

King, S. M., Butcher, A. C., Rosenoern, T., Coz, E., Lieke, K. I., de Leeuw, G., et al. (2012). Investigating primary marine aerosol properties: CCN Activity of sea salt and mixed inorganic organic particles. *Environmental Science & Technology*, *46*(19), 10,405–10,412. https://doi.org/10.1021/es300574u

Kirpes, R. M., Bonanno, D., May, N. W., Fraund, M., Barget, A. J., Moffet, R. C., et al. (2019). Wintertime Arctic sea spray aerosol composition controlled by sea ice lead microbiology. *ACS Central Science*, *5*(11), 1760–1767. https://doi.org/10.1021/acscentsci.9b00541

Kirpes, R. M., Bondy, A. L., Bonanno, D., Moffet, R. C., Wang, B., Laskin, A., et al. (2018). Secondary sulfate is internally mixed with sea spray aerosol and organic aerosol in the winter Arctic. *Atmospheric Chemistry and Physics*, *18*(6), 3937–3949. https://doi.org/10.5194/acp-18-3937-2018

Kooistra, W. H. C. F., Sarno, D., Balzano, S., Gu, H., Andersen, R. A., & Zingone, A. (2008). Global diversity and biogeography of skeletonema species (Bacillariophyta). *Protist*, *159*(2), 177–193. https://doi.org/10.1016/j.protis.2007.09.004

Lange, R., Dall'Osto, M., Skov, H., N∅jgaard, J. K., Nielsen, I. E., Beddows, D. C. S., et al. (2018). Characterization of distinct Arctic aerosol accumulation modes and their sources. *Atmospheric Environment*, *183*, 1–10. https://doi.org/10.1016/j.atmosenv.2018.03.060

Lange, R., Dall'Osto, M., Wex, H., Skov, H., & Massling, A. (2019). Large summer contribution of organic biogenic aerosols to Arctic cloud condensation nuclei. *Geophysical Research Letters*, *46*, 11,500–11,509. https://doi.org/10.1029/2019GL084142

Leck, C., & Bigg, E. K. (2005a). Biogenic particles in the surface microlayer and overlaying atmosphere in the central Arctic Ocean during summer. *Tellus B: Chemical and Physical Meteorology*, *57*(4), 305–316. https://doi.org/10.3402/tellusb.v57i4.16546

Leck, C., & Bigg, E. K. (2005b). Source and evolution of the marine aerosol—A new perspective. *Geophysical Research Letters*, *32*, L19803. https://doi.org/10.1029/2005GL023651

Leck, C., & Svensson, E. (2015). Importance of aerosol composition and mixing state for cloud droplet activation over the Arctic pack ice in summer. *Atmospheric Chemistry and Physics*, *15*(5), 2545–2568. https://doi.org/10.5194/acp-15-2545-2015

Lewis, E. R., & Schwartz, S. E. (2004). *Sea salt aerosol production: Mechanisms, methods, measurements, and models—A critical review*: American Geophysical Union.

Loewe, K., Ekman, A. M. L., Paukert, M., Sedlar, J., Tjernström, M., & Hoose, C. (2017). Modelling micro- and macrophysical contributors to the dissipation of an Arctic mixed-phase cloud during the Arctic Summer Cloud Ocean Study (ASCOS). *Atmospheric Chemistry and Physics*, *17*(11), 6693–6704. https://doi.org/10.5194/acp-17-6693-2017

Lohmann, U., & Feichter, J. (2005). Global indirect aerosol effects: A review. *Atmospheric Chemistry and Physics*, *5*(3), 715–737. https://doi.org/10.5194/acp-5-715-2005

Möhler, O., Benz, S., Saathoff, H., Schnaiter, M., Wagner, R., Schneider, J., et al. (2008). The effect of organic coating on the heterogeneous ice nucleation efficiency of mineral dust aerosols. *Environmental Research Letters*, *3*, 025007. https://doi.org/10.1088/1748-9326/3/2/025007

Möhler, O., Stetzer, O., Schaefers, S., Linke, C., Schnaiter, M., Tiede, R., et al. (2003). Experimental investigation of homogeneous freezing of sulphuric acid particles in the aerosol chamber AIDA. *Atmospheric Chemistry and Physics*, *3*(1), 211–223.

Martin, M., Chang, R. Y.-W., Sierau, B., Sjogren, S., Swietlicki, E., Abbatt, J. P. D., et al. (2011). Cloud condensation nuclei closure study on summer arctic aerosol. *Atmospheric Chemistry and Physics*, *11*(22), 11,335–11,350. https://doi.org/10.5194/acp-11-11335-2011

Moore, M. J. K., Furutani, H., Roberts, G. C., Moffet, R. C., Gilles, M. K., Palenik, B., & Prather, K. A. (2011). Effect of organic compounds on cloud condensation nuclei (CCN) activity of sea spray aerosol produced by bubble bursting. *Atmospheric Environment*, *45*(39), 7462–7469. https://doi.org/10.1016/j.atmosenv.2011.04.034

Morrison, H., & Grabowski, W. W. (2008). Modeling supersaturation and subgrid-scale mixing with two-moment bulk warm microphysics. *Journal of the Atmospheric Sciences*, *65*(3), 792–812. https://doi.org/10.1175/2007JAS2374.1

Morrison, H., Zuidema, P., Ackerman, A. S., Avramov, A., de Boer, G., Fan, J., et al. (2011). Intercomparison of cloud model simulations of Arctic mixed-phase boundary layer clouds observed during SHEBA/FIRE-ACE. *Journal of Advances in Modeling Earth Systems*, *3*, M05001. https://doi.org/10.1029/2011MS000066

Murray, B. J., O'Sullivan, D., Atkinson, J. D., & Webb, M. E. (2012). Ice nucleation by particles immersed in supercooled cloud droplets. *Chemical Society Reviews*, *41*(19), 6519–6554. https://doi.org/10.1039/c2cs35200a

Nguyen, Q. T., Kjær, K. H., Kling, K. I., Boesen, T., & Bilde, M. (2017). Impact of fatty acid coating on the CCN activity of sea salt particles. *Tellus B: Chemical and Physical Meteorology*, *69*(1), 1,304,064. https://doi.org/10.1080/16000889.2017.1304064

Orellana, M. A., Matrai, P. A., Leck, C., Rauschenberg, C. D., Lee, A. M., & Coz, E. (2011). Marine microgels as a source of cloud condensation nuclei in the high Arctic. *Proceedings of the National Academy of Sciences*, *108*(33), 13,612 LP–13,617. https://doi.org/10.1073/pnas.1102457108

Ovadnevaite, J., Zuend, A., Laaksonen, A., Sanchez, K. J., Roberts, G., Ceburnis, D., et al. (2017). Surface tension prevails over solute effect in organic-influenced cloud droplet activation. *Nature*, *546*, 637–641.

Petters, M. D., & Kreidenweis, S. M. (2007). A single parameter representation of hygroscopic growth and cloud condensation nucleus activity. *Atmospheric Chemistry and Physics*, *7*(8), 1961–1971. https://doi.org/10.5194/acp-7-1961-2007

Prenni, A. J., Harrington, J. Y., Tjernström, M., DeMott, P. J., Avramov, A., Long, C. N., et al. (2007). Can ice-nucleating aerosols affect arctic seasonal climate?. *Bulletin of the American Meteorological Society*, *88*(4), 541–550. https://doi.org/10.1175/BAMS-88-4-541

Prisle, N. L., Raatikainen, T., Laaksonen, A., & Bilde, M. (2010). Surfactants in cloud droplet activation: Mixed organic-inorganic particles. *Atmospheric Chemistry and Physics*, *10*(12), 5663–5683. https://doi.org/10.5194/acp-10-5663-2010

Quinn, P. K., Collins, D. B., Grassian, V. H., Prather, K. A., & Bates, T. S. (2015). Chemistry and related properties of freshly emitted sea spray aerosol. *Chemical Reviews*, *115*(10), 4383–4399. https://doi.org/10.1021/cr500713g

Rasmussen, B. B., Nguyen, Q. T., Kristensen, K., Nielsen, L. A. S., & Bilde, M. (2017). What controls volatility of sea spray aerosol? Results from laboratory studies using artificial and real seawater samples. *Journal of Aerosol Science*, *107*, 134–141. https://doi.org/10.1016/j.jaerosci.2017.02.002

Renbaum-Wolff, L., Song, M., Marcolli, C., Zhang, Y., Liu, P. F., Grayson, J. W., et al. (2016). Observations and implications of liquid-liquid phase separation at high relative humidities in secondary organic material produced by α-pinene ozonolysis without inorganic salts. *Atmospheric Chemistry and Physics*, *16*(12), 7969–7979. https://doi.org/10.5194/acp-16-7969-2016

Rose, D., Gunthe, S. S., Mikhailov, E., Frank, G. P., Dusek, U., Andreae, M. O., & Pöschl, U. (2008). Calibration and measurement uncertainties of a continuous-flow cloud condensation nuclei counter (DMT-CCNC): CCN activation of ammonium sulfate and sodium chloride aerosol particles in theory and experiment. *Atmospheric Chemistry and Physics*, *8*(5), 1153–1179. https://doi.org/10.5194/acp-8-1153-2008

Savre, J., Ekman, A. M. L., & Svensson, G. (2014). Technical note: Introduction to MIMICA, a large-eddy simulation solver for cloudy planetary boundary layers. *Journal of Advances in Modeling Earth Systems*, *6*, 630–649. https://doi.org/10.1002/2013MS000292

Schmale, J., Henning, S., Decesari, S., Henzing, B., Keskinen, H., Sellegri, K., et al. (2018). Long-term cloud condensation nuclei number concentration, particle number size distribution and chemical composition measurements at regionally representative observatories. *Atmospheric Chemistry and Physics*, *18*(4), 2853–2881. https://doi.org/10.5194/acp-18-2853-2018

Schnell, R. C., & Vali, G. (1975). Freezing nuclei in marine waters. *Tellus*, *27*(3), 321–323. https://doi.org/10.3402/tellusa.v27i3.9911

Seifert, A., & Beheng, K. D. (2001). A double-moment parameterization for simulating autoconversion, accretion and selfcollection. *Atmospheric Research*, *59-60*, 265–281. https://doi.org/10.1016/S0169-8095(01)00126-0

Seinfeld, J. H., & Pandis, S. N. (2016). *Atmospheric chemistry and physics: From air pollution to climate change* (3rd ed.). Hoboken, NJ: John Wiley & Sons.

Shupe, M. D., & Intrieri, J. M. (2004). Cloud radiative forcing of the Arctic surface: The influence of cloud properties, surface albedo, and solar zenith angle. *Journal of Climate*, *17*(3), 616–628. https://doi.org/10.1175/1520-0442(2004)017<0616:CRFOTA>2.0.CO;2

Shupe, M. D., Persson, P. O. G., Brooks, I. M., Tjernström, M., Sedlar, J., Mauritsen, T., et al. (2013). Cloud and boundary layer interactions over the Arctic sea ice in late summer. *Atmospheric Chemistry and Physics*, *13*(18), 9379–9399. https://doi.org/10.5194/acp-13-9379-2013

Silvergren, S., Wideqvist, U., Ström, J., Sjogren, S., & Svenningsson, B. (2014). Hygroscopic growth and cloud forming potential of Arctic aerosol based on observed chemical and physical characteristics (a 1 year study 2007–2008). *Journal of Geophysical Research: Atmospheres*, *119*, 14–80. https://doi.org/10.1002/2014JD021657

Stevens, R. G., Loewe, K., Dearden, C., Dimitrelos, A., Possner, A., Eirund, G. K., et al. (2018). A model intercomparison of CCN-limited tenuous clouds in the high Arctic. *Atmospheric Chemistry and Physics*, *18*(15), 11,041–11,071. https://doi.org/10.5194/acp-18-11041-2018

Struthers, H., Ekman, A. M. L., Glantz, P., Iversen, T., Kirkevåg, A., Mårtensson, E. M., et al. (2011). The effect of sea ice loss on sea salt aerosol concentrations and the radiative balance in the Arctic. *Atmospheric Chemistry and Physics*, *11*(7), 3459–3477. https://doi.org/10.5194/acp-11-3459-2011

Tjernström, M., Leck, C., Birch, C. E., Bottenheim, J. W., Brooks, B. J., Brooks, I. M., et al. (2014). The Arctic Summer Cloud Ocean Study (ASCOS): Overview and experimental design. *Atmospheric Chemistry and Physics*, *14*(6), 2823–2869. https://doi.org/10.5194/acp-14-2823-2014

Topping, D., Barley, M., Bane, M. K., Higham, N., Aumont, B., Dingle, N., & McFiggans, G. (2016). UManSysProp v1.0: An online and open-source facility for molecular property prediction and atmospheric aerosol calculations. *Geoscientific Model Development*, *9*(2), 899–914. https://doi.org/10.5194/gmd-9-899-2016

Wagner, R., Bunz, H., Linke, C., Möhler, O., Naumann, K.-H., Saathoff, H., et al. (2006). Chamber simulations of cloud chemistry: The AIDA chamber. In Barnes, I., & Rudzinski, K. J. (Eds.), *Environmental simulation chambers: Application to atmospheric chemical processes* (pp. 67–82). Dordrecht: Springer Netherlands. https://doi.org/10.1007/1-4020-4232-9_5

Wagner, R., Möhler, O., & Schnaiter, M. (2012). Infrared optical constants of crystalline sodium chloride dihydrate: Application to study the crystallization of aqueous sodium chloride solution droplets at low temperatures. *The Journal of Physical Chemistry A*, *116*(33), 8557–8571. https://doi.org/10.1021/jp306240s

Wex, H., Fuentes, E., Tsagkogeorgas, G., Voigtländer, J., Clauss, T., Kiselev, A., et al. (2010). The influence of algal exudate on the hygroscopicity of sea spray particles. *Advances in Meteorology*, *2010*, 365131. https://doi.org/10.1155/2010/365131

Wilson, T. W., Ladino, L. A., Alpert, P. A., Breckels, M. N., Brooks, I. M., Browse, J., et al. (2015). A marine biogenic source of atmospheric ice-nucleating particles. *Nature*, *525*(7568), 234–238. https://doi.org/10.1038/nature14986

Wurl, O., Wurl, E., Miller, L., Johnson, K., & Vagle, S. (2011). Formation and global distribution of sea-surface microlayers. *Biogeosciences*, *8*, 121–135. https://doi.org/10.5194/bg-8-121-2011

Xu, L., Russell, L. M., Somerville, R. C. J., & Quinn, P. K. (2013). Frost flower aerosol effects on Arctic wintertime longwave cloud radiative forcing. *Journal of Geophysical Research: Atmospheres*, *118*, 13,282–13,291. https://doi.org/10.1002/2013JD020554

Zábori, J., Rastak, N., Yoon, Y. J., Riipinen, I., & Ström, J. (2015). Size-resolved cloud condensation nuclei concentration measurements in the Arctic: Two case studies from the summer of 2008. *Atmospheric Chemistry and Physics*, *15*(23), 13,803–13,817. https://doi.org/10.5194/acp-15-13803-2015

Zieger, P., Väisänen, O., Corbin, J. C., Partridge, D. G., Bastelberger, S., Mousavi-Fard, M., et al. (2017). Revising the hygroscopicity of inorganic sea salt particles. *Nature Communications*, *8*, ncomms15883. https://doi.org/10.1038/ncomms15883